

Role of TiO₂ nanoparticles on the photoinduced intramolecular electron-transfer reaction within a novel synthesized donor–acceptor system

S.K. Pal^a, S. Bhattacharaya^a, S.K. Batabyal^b, T.K. Pradhan^c, T. Ganguly^{a,*}

^a Department of Spectroscopy, Indian Association for the Cultivation of Science, 2A & B Raja S C Mullick Road, Jadavpur, Kolkata 700032, India

^b Department of Solid State Physics, Indian Association for the Cultivation of Science, 2A & B Raja S C Mullick Road, Jadavpur, Kolkata 700032, India

^c Department of Organic Chemistry, Indian Association for the Cultivation of Science, 2A & B Raja S C Mullick Road, Jadavpur, Kolkata 700032, India

Received 30 July 2006; received in revised form 26 December 2006; accepted 15 January 2007

Available online 19 January 2007

Abstract

Steady-state, FT-IR and time-resolved spectroscopic measurements were carried out on the two novel synthesized π -conjugated rigid naphthothiophene compounds, 7-methoxynaphtho[1,2-*b*]thiophene (7MNT) and 7-methoxynaphtho[1,2-*b*]thiophene-2-carboxylic acid (7MTCA) in chloroform (CHCl₃) medium as well as in presence of TiO₂ nanoparticles. 7MTCA multichromophoric system contains both electron donor (–OCH₃) and acceptor functionalities (–COOH) at the two different ends of the rigid naphthothiophene moiety whereas in 7MNT only the electron donor functional group, –OCH₃, is present. Thus 7MNT looks like the donor part of 7MTCA where –COOH group overlaps, due to its free rotation, with the electron rich site 7MNT part. The experimental findings observed from steady-state absorption, fluorescence and time-resolved spectroscopic (fluorescence lifetime and transient absorption) measurements demonstrate that the survival duration of charge-separated species formed within 7MTCA due to intramolecular photoinduced electron-transfer (PET) reactions between the donor –OCH₃ and acceptor –COOH functional groups, attached at the two different ends of this compound, could be enhanced by inhibiting the energy wasting charge recombination process through complexation of the carboxylate group (–COOH) with TiO₂ nanoparticles. Thus, in the present investigation TiO₂ appears not to act as an acceptor but its presence helps to survive or protect the charge-separated species formed within 7MTCA. The possibility of designing of low-cost artificial (model) solar energy conversion devices by linking the organic donor–acceptor (DA) systems like 7MTCA with TiO₂ core is hinted.

© 2007 Elsevier B.V. All rights reserved.

Keywords: Charge separation; Charge recombination; Laser flash photolysis; TiO₂ nanoparticles; Naphthothiophene; FT-IR

1. Introduction

In contemporary materials research, organic–inorganic nanocomposites become a highly exciting area [1–6]. This type of research possesses immense importance not only from the basic research point of view but it has strong technological relevance, e.g., for constructing light emitting diodes, photovoltaic cells, future solar cells, etc. [7–15]. The key process involved in the solar cells is a photoinduced electron-transfer (PET) between the organic molecules and the nanocrystalline inorganic phase to generate the charge carriers [16,17]. Lately to develop

systems which act as both light-absorbing dye and a charge transport materials, attempts are made to combine nanocrystalline semiconductors like TiO₂, CdSe, ZnO, etc., with π -conjugated organic or polymer systems [18–20]. Some authors reported the PET process in heterosupramolecular assemblies of nanostructured TiO₂ or other similar nanocrystalline semiconductors (like ZnO, SnO₂, etc.) and various donor–acceptor contained organic molecules including the systems having the carboxylate group, –COOH [7,21–30].

Our primary objective is to investigate the interaction of TiO₂ nanoparticles in chloroform (CHCl₃) solvent with π -conjugated rigid naphthothiophene system, 7-methoxynaphtho[1,2-*b*]thiophene-2-carboxylic acid (7MTCA), containing both the donor (–OCH₃) and acceptor (–COOH) functionalities at the two different ends of the naphthothiophene moiety (Fig. 1).

* Corresponding author. Tel.: +91 33 2473 4971x253; fax: +91 33 2473 2805.
E-mail address: tapcla@rediffmail.com (T. Ganguly).

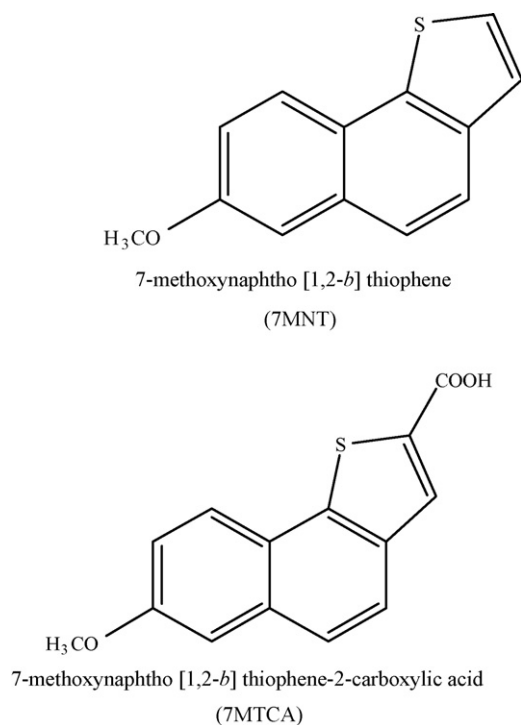


Fig. 1. Molecular structures of the compounds 7MNT and 7MTCA.

As $-\text{COOH}$ group is known to have a strong binding affinity, through hydrogen bonding or other mechanisms like formation of bidentate complex, with TiO_2 nanosurface, the present investigations were made to see whether such type of binding in the ground state has some effects on the charge-separated species formed due to photoinduced electron-transfer reactions between the donor and acceptor functional groups. Attempts are also made to examine whether survival duration of the charge-separated species could be enhanced by retarding the energy wasting charge recombination process through binding mechanisms of TiO_2 with the acceptor functionality $-\text{COOH}$ which is generally employed as an anchor to the semiconductor nanosurface [8]. To understand more clearly the photophysical properties of 7MTCA, the similar investigations were also made on 7-methoxynaphtho[1,2-*b*]thiophene (7MNT) where no $-\text{COOH}$ group is present but it contains only the donor functionality $-\text{OCH}_3$. Thus, 7MNT behaves as a donor part of the other multichromophoric system, 7MTCA. Our primary aim of the present investigation is to develop some nanocomposite systems of organic solutes being attached with TiO_2 nanoparticles. These simple nanocomposite systems have an advantage over various triads, tetrads, pentad systems to produce charge-separated states having prolonged lifetime. In donor-acceptor multichromophoric systems, considerable energies are lost during the multi-step electron-transfer processes in artificial long-range charge separation. Thus to design low cost hetero-supramolecular assemblies for solar-energy conversion devices, avoidances of such energy wasting and high-cost multi-step synthesis are absolutely necessary. The results obtained from the steady-state and time-resolved spectroscopic investigations on this simple rigid naphthothiophene system

7MTCA, containing both the donor and acceptor functionalities, in presence of TiO_2 nanoparticles are described in this paper.

2. Experimental

2.1. Materials

The synthesis and characterization of the compounds 7-methoxynaphtho[1,2-*b*]thiophene (7MNT) and 7-methoxynaphtho[1,2-*b*]thiophene-2-carboxylic acid (7MTCA) have been described elsewhere [31]. Chloroform (CHCl_3) (E. Merck, Germany) of spectroscopic grade was used as received.

2.2. Preparation of TiO_2 nanoparticles

Nanocrystals of TiO_2 were prepared by arrested hydrolysis of titanium isopropoxide (TIP) in anhydrous chloroform (CHCl_3) containing a little amount of 1-propanol and double distilled water in presence of the stabilizer stearic acid following the method described by Janssen and Beek [8a]. In a typical synthesis we take a reaction mixture containing 50 ml CHCl_3 , 1.5 ml 1-propanol, 0.05 ml TIP and 0.044 gm stearic acid. Another reaction mixture were prepared by mixing 1 ml 1-propanol and 8 μl double distilled water which were then added with the 1st reaction mixture drop wise with constant stirring. A clear solution of TiO_2 nanoparticles stabilized by stearic acid were obtained after 24 h. Then TiO_2 nanoparticles were precipitated by adding acetonitrile to the above solution separated by centrifugation and washed with ethanol several time and finally vacuum dried at 60 °C for 24 h. The UV-vis spectroscopy can be used to determine the diameter of semiconductor nanoparticle due to its quantum-confined phenomena. The UV-vis spectrum of nanoparticles in chloroform shows an absorption onset at about 340 nm. According to the earlier reports [32,33], an onset at 340 nm implies the average particle diameter of about 2 nm. Colloidal TiO_2 solution was prepared by dissolving the desired amount of TiO_2 particles into chloroform (CHCl_3). The size of the TiO_2 nanoparticles was also estimated from high resolution Transmission Electron Micrograph (TEM) as shown in Fig. 2. The particle diameter varies in the range of 2–4 nm. The average diameter of TiO_2 nanoparticle is found to be 4 nm.

2.3. Spectroscopic apparatus

At the ambient temperature (296 K), steady-state electronic absorption and fluorescence emission spectra of dilute solutions (10^{-4} to 10^{-6} mol dm^{-3}) of the samples were recorded using a 1 cm path length rectangular quartz cells by means of an absorption spectrophotometer (Shimadzu UV-vis 2101PC) and F-4500 fluorescence spectrophotometer (Hitachi), respectively. FT-IR spectra were recorded by using a FTIR 8400S Shimadzu spectrometer. Fluorescence lifetime measurements were carried out using the Time Master fluorimeter from Photon Technology International (PTI). The system measures fluorescence lifetimes using PTI's patented strobe technique and

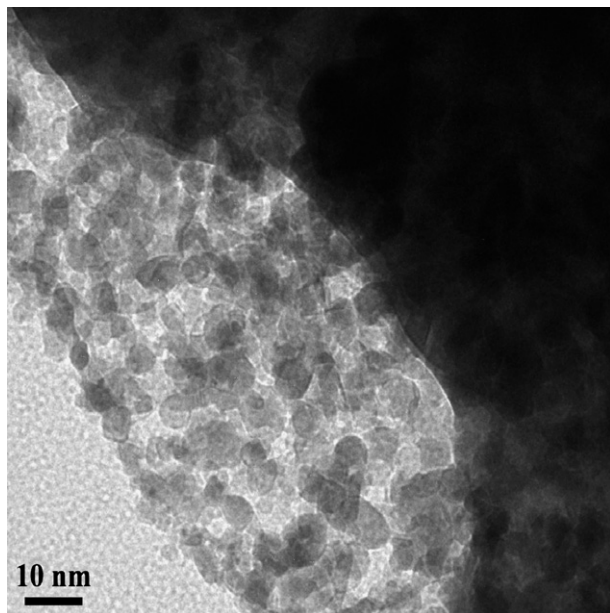


Fig. 2. TEM picture of TiO₂ nanoparticles.

gated detection. The software FeliX32 controls all acquisition modes and data analysis of the Time Master system. The sample was excited using a thyatron gated Nitrogen flash lamp (width ~ 2 ns) capable of measuring fluorescence time-resolved acquisitions at a flash rate of 25 KHz. The quality of fit has been assessed over the entire decay, including the rising edge, and tested with a plot of weighted residuals, the other statistical parameters, e.g., the reduced χ^2 and the Darbin–Watson parameters. All the solutions for room temperature measurements were deoxygenated by purging with argon gas stream for about 30 min.

2.4. Laser flash photolysis

Transient absorption spectra were measured using nanosecond flash photolysis set-up (Applied Photophysics) containing a Nd:YAG laser (DCR-11, Spectra Physics) (laser fluence ~ 13 mJ cm⁻²). The samples were excited by 355 nm laser light (FWHM = 8 ns). Triplet spectra were monitored through absorption light from a pulsed Xe lamp (250 W). The photomultiplier (IP28) output was fed into a combiscope (Fluke PM3394B, 200 MHz) and the data were analyzed using Fluke View Combiscope software.

2.5. Electrochemical measurements

The redox potentials were measured in acetonitrile solvent by cyclic voltammetric method using the PAR model VersaStat II electrochemistry system. Three electrode systems including Ag/AgCl as standard were used in the measurements. Tetraethylammonium perchlorate (TEAP) was used as the supporting electrolyte. The oxidized species of 7MNT has been prepared by constant current charger (model DB 300 DB Electronics, India).

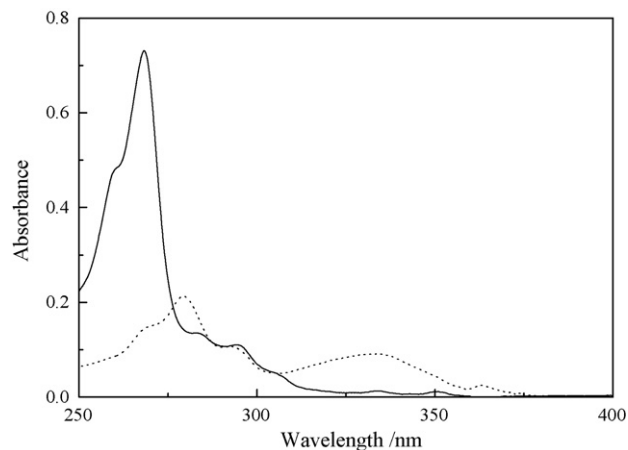


Fig. 3. Steady-state UV–vis absorption spectra of 7MNT (solid line) (conc. $\sim 5 \times 10^{-6}$ mol dm⁻³) and 7MTCA (dotted line) (conc. $\sim 4.12 \times 10^{-5}$ mol dm⁻³) in CHCl₃.

3. Results and discussion

3.1. Steady-state (UV–vis and FT-IR) studies

The steady-state UV–vis absorption spectra of the molecule 7MNT (containing only the donor functional group OCH₃) and the donor–acceptor (DA) system 7MTCA, in chloroform (CHCl₃) were measured and shown in Fig. 3. In the DA system, not only the absorption maximum of the donor part is shifted, but also a new broad band peaking at 340 nm and extending up to 375 nm is observed. The additional band in the DA system possesses the typical features of charge-transfer (CT) transition and indicates the presence of appreciable interaction in the ground state between the donor and acceptor sites of the DA system 7MTCA.

Fig. 4 shows the absorption spectra of 7MTCA in CHCl₃ and the effect of increasing the TiO₂ concentration. Every time, the

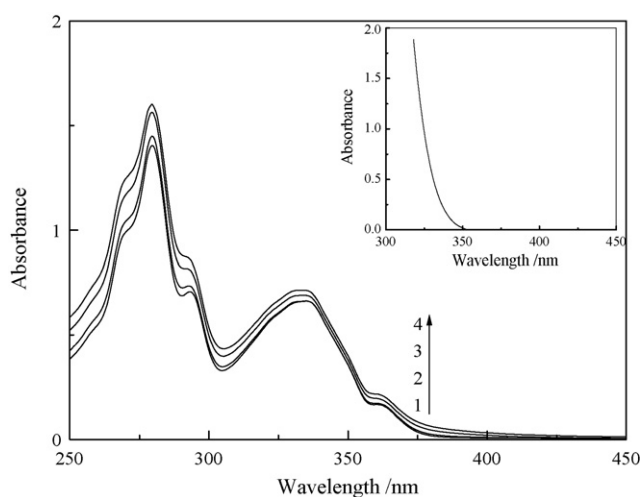


Fig. 4. UV–vis absorption spectra of 7MTCA (conc. $\sim 2.3 \times 10^{-5}$ mol dm⁻³) in CHCl₃ in the presence of TiO₂ nanoparticles: (1) 0 mol dm⁻³; (2) 1.34×10^{-5} mol dm⁻³; (3) 3.98×10^{-5} mol dm⁻³; (4) 5.29×10^{-5} mol dm⁻³. (Inset) UV–vis spectra of the TiO₂ colloidal solution (conc. $\sim 3.4 \times 10^{-3}$ mol dm⁻³) in CHCl₃.

mixture of 7MTCA and TiO₂ was prepared by adding desired amount of colloidal solution of TiO₂ into the solution of 7MTCA in CHCl₃ and then sonicated for 30 min at 30° C. With the addition of TiO₂ nanoparticles, the entire absorption spectra undergo a hyperchromic effect without any noticeable spectral shift. As the shape of the CT absorption band and its position remain unaltered with addition of TiO₂, it is apparent that the possibility of complex formation of 7MTCA with TiO₂ is very slim. It shows that TiO₂ simply modifies the CT absorption band of 7MTCA without undergoing CT interaction with the organic solute. The change of absorption with TiO₂ concentration at a fixed wavelength was analyzed by using the Langmuir adsorption isotherm [16,17] and an association constant of $K_a = 5 \times 10^4 \text{ M}^{-1}$ between 7MTCA and TiO₂ nanoparticle was estimated from the well-known Benesi–Hildebrand plot. The observed high association constant along with the spectral changes indicates a strong interaction between the DA system and the TiO₂ nanoparticle in the ground state and the formation of ground surface complexes between the two. The most likely interaction model between the 7MTCA and TiO₂ particles is that the COOH/COO⁻ group of 7MTCA molecule coordinates either directly or through a hydrogen bond to the TiO₂ surface [34,35]. With 7MNT molecule, which contains only donor group and no acceptor being present unlike 7MTCA, no such hyperchromic effect was found in presence of TiO₂ which further confirms the possibility of complexation of carboxylate group of 7MTCA with TiO₂ nanoparticles. UV–vis measurements of a synthesized compound, 5-nitro-benzo[*b*]thiophene-2-carboxylic acid which contains no –OCH₃ donor functionality but only acceptor groups –NO₂ and –COOH at both the ends of the rigid benzothiophene moiety, reveal that no charge-transfer band is apparent unlike the presently studied molecule 7MTCA where both donor and acceptor groups are present. Thus, the direct participation of the donor functionality (–OCH₃) in charge-transfer reactions with the acceptor group –COOH is confirmed. However, as UV–vis measurement is not enough to investigate the molecular structure of adsorbed molecules (7MTCA and TiO₂), Fourier transform infrared (FT-IR) technique was used to gain further information about the nature of binding of the DA system 7MTCA with TiO₂ surface.

Fig. 5a shows the FT-IR spectra of stearic acid (solid line) and TiO₂ coated with stearic acid (broken line). The C–H stretching vibrations of the alkyl chain of stearic acid are observed in both the spectra of Fig. 5a between 2849 and 2955 cm⁻¹. The spectrum of pure stearic acid shows the C=O stretching vibration at 1703 cm⁻¹. This band is completely converted into the three new bands in the spectrum of the stearic acid coated with TiO₂ nanoparticles. The new bands at 1630, 1530 and 1445 cm⁻¹ originate from carboxylate binding to the TiO₂ surface [8a]. Fig. 5b exhibits the FT-IR spectra of 7MTCA (broken line) and 7MTCA binded TiO₂ nanoparticles (solid line). It is apparent from Fig. 5b that the C=O stretching vibration of 7MTCA resides at 1670 cm⁻¹. This band completely disappears in the spectrum of 7MTCA binded with TiO₂ nanoparticles and converted into the three bands at 1622, 1533 and 1464 cm⁻¹. A few side bands also develop in the FT-IR spectra of binded 7MTCA with TiO₂. These bands were absent in the spectrum of

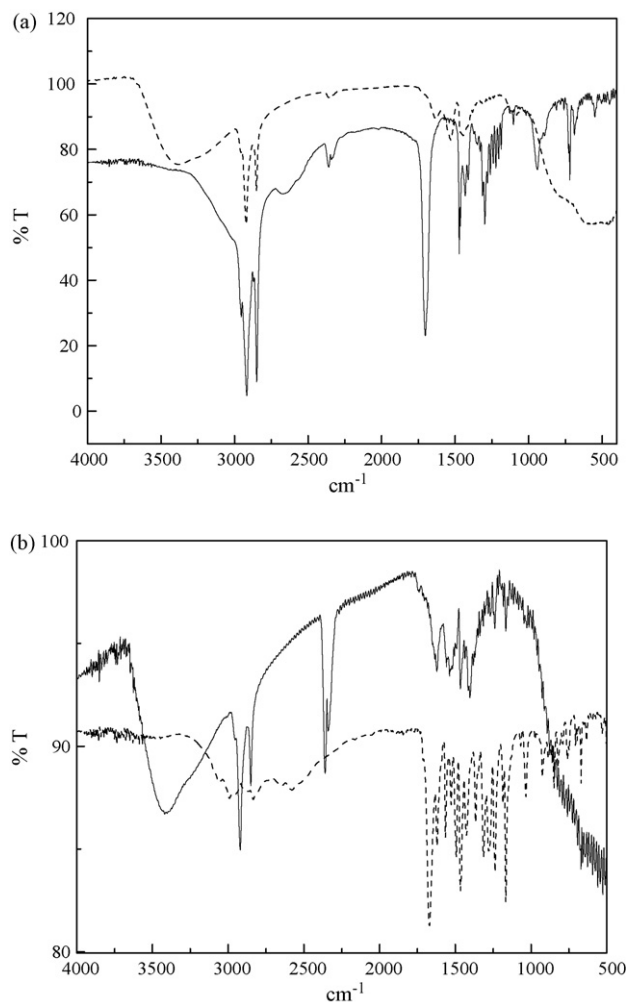


Fig. 5. (a) FT-IR spectra of stearic acid (solid line) and TiO₂ coated with stearic acid (broken line). (b) FT-IR spectra of 7MTCA (broken line) and 7MTCA binded TiO₂ nanoparticles (solid line).

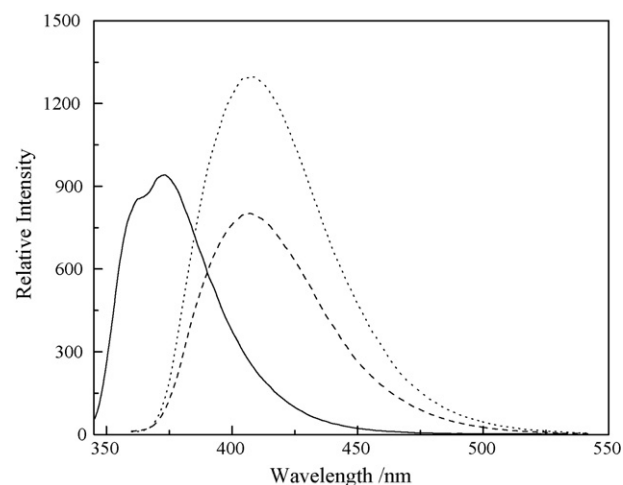


Fig. 6. Fluorescence emission spectra of 7MNT (conc. $\sim 5 \times 10^{-6} \text{ mol dm}^{-3}$) with excitation wavelength $\sim 305 \text{ nm}$ (solid line), 7MTCA (conc. $\sim 4.12 \times 10^{-5} \text{ mol dm}^{-3}$) with excitation wavelength $\sim 305 \text{ nm}$ (dashed line) and 340 nm (dotted line) in CHCl₃.

Table 1
Time-resolved fluorescence data in CHCl_3 (f_i , fractional contribution) at the ambient temperature

System	λ_{ex} (nm)	λ_{em} (nm)	τ_1 (ns)	f_1	τ_2 (ns)	f_2	χ^2
7MNT	297	370	0.7	1.0	–	–	1.01
7MTCA	297	370	0.34	0.61	2.4	0.39	1.03
7MTCA	297	425	0.34	0.26	2.4	0.74	1.07
7MTCA	375	410	0.34	0.47	2.4	0.53	1.04
7MTCA + TiO ₂	375	410	0.34	0.46	2.4	0.54	1.03

The monoexponential decay: $I(\lambda, t) = A \exp(-t/\tau)$. The biexponential decay: $I(\lambda, t) = A_1 \exp(-t/\tau_1) + A_2 \exp(-t/\tau_2)$, $f_i = A_i \tau_i / (\sum_j A_j \tau_j)$.

stearic acid coated with TiO₂. From these observations it reveals that 7MTCA is attached with the TiO₂ surface via carboxylate binding.

3.2. Steady-state and time-resolved fluorescence

The steady-state fluorescence emission spectra of 7MNT and 7MTCA in chloroform are reproduced in Fig. 6. On excitation of 7MTCA at the isosbestic point [36] it was observed that the fluorescence emission band of 7MNT spanning between 340 and 475 nm, was somehow quenched and a new long wavelength band peaking at 410 nm appeared. On the other hand, a fluorescence band of considerable intensity with the same energy maximum (~410 nm) was found after excitation at the CT absorption band of 7MTCA at 340 nm. It is apparent from this observation that the band at 410 nm should be the CT emission band whose formation is largely facilitated in system containing donor and acceptor sites [37].

The time-resolved fluorescence data (Table 1) shows that the fluorescence decay of the donor 7MNT is monoexponential with lifetime 0.7 ns, but the fluorescence decay of 7MTCA is biexponential with lifetimes 0.34 and 2.4 ns. As the monitoring wavelength of 7MTCA changes from shorter wavelength side (370 nm) to longer wavelength side (425 nm) of the emission band, the fractional contribution of the short lived component (0.34 ns) decreases with the increase of the contribution of longer lived one (2.4 ns). From these observations it is apparent that the short and longer component should correspond to the quenched lifetime of the donor and the lifetime of the CT fluorescence, respectively. As at 355 nm TiO₂ has no absorption at $10^{-5} \text{ mol dm}^{-3}$ concentration, which was used for fluorescence lifetime measurements (inset of Fig. 4 is for TiO₂ at $\sim 10^{-3} \text{ mol dm}^{-3}$), only 7MTCA gets excited by this wavelength and the possibility of formation of valence band holes and conduction band electron is very slim as TiO₂ remains unexcited.

Assuming that the fluorescence quenching totally originates from the singlet electron-transfer, the rate constant, k_{SET} and efficiency, ϕ_{SET} of intramolecular electron-transfer were determined using Eqs. (1) and (2) [38]:

$$k_{\text{SET}} = \frac{1}{\tau} - \frac{1}{\tau_0} \quad (1)$$

$$\phi_{\text{SET}} = 1 - \frac{\tau}{\tau_0} \quad (2)$$

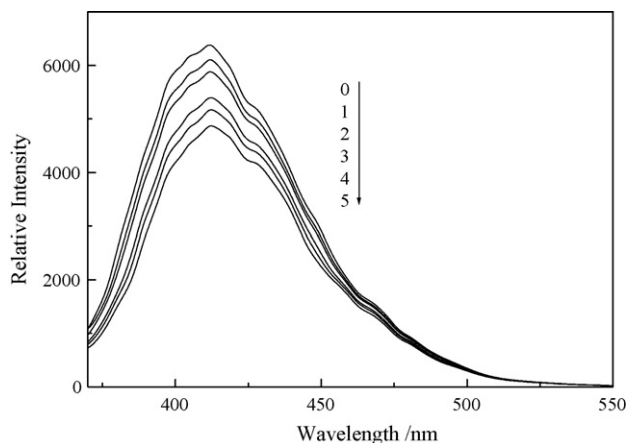


Fig. 7. Fluorescence emission spectra of 7MTCA (conc. $\sim 2.3 \times 10^{-5} \text{ mol dm}^{-3}$) ($\lambda_{\text{ex}} = 355 \text{ nm}$) in CHCl_3 in the presence of TiO₂ nanoparticles: (0) 0; (1) $1.34 \times 10^{-5} \text{ mol dm}^{-3}$; (2) $2.67 \times 10^{-5} \text{ mol dm}^{-3}$; (3) $5.29 \times 10^{-5} \text{ mol dm}^{-3}$; (4) $6.59 \times 10^{-5} \text{ mol dm}^{-3}$; (5) $7.87 \times 10^{-5} \text{ mol dm}^{-3}$.

where τ_0 and τ are the unquenched and quenched lifetimes of the donor, respectively. k_{SET} and ϕ_{SET} were obtained to be $\sim 1.5 \times 10^9 \text{ s}^{-1}$ and ~ 0.51 , respectively.

Fig. 7 shows the CT emission spectra of 7MTCA in the presence of varying amounts of TiO₂ nanoparticles. Addition of colloidal solution of TiO₂ to a solution of the DA system 7MTCA resulted in the quenching of CT fluorescence of the DA system 7MTCA. The quenching of emission spectra of 7MTCA in the presence of TiO₂ nanoparticles exhibits upward curvature in Stern–Volmer (SV) plot (Fig. 8). This non-linear behavior of SV plot may be due to the domination of static mode in the quenching reaction mechanism [39]. On the other hand, the fluorescence lifetimes of 7MTCA in CHCl_3 remain unaffected with the addition of TiO₂ nanoparticles (Table 1). This observation rules out the possibilities of the presence of any dynamic quenching mode in the observed quenching phenomena of CT band of 7MTCA. The static nature of quenching mode also supports our presumption on the formation of ground surface complexes between

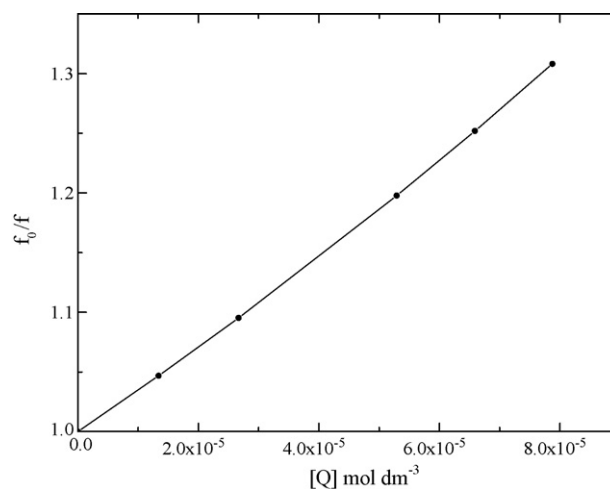


Fig. 8. Stern–Volmer (SV) plot from steady-state fluorescence emission intensity measurements in the case of 7MTCA in the presence of TiO₂ in CHCl_3 fluid solution.

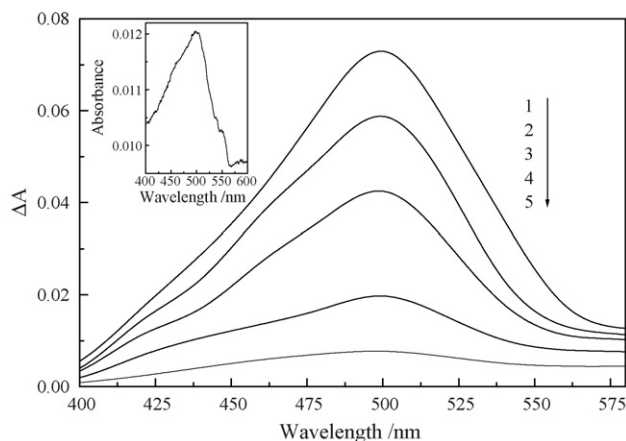


Fig. 9. Transient absorption spectra of 7MTCA (excitation wavelength ~ 355 nm) at the ambient temperature at delay times: (1) 4 μ s; (2) 5 μ s; (3) 6 μ s; (4) 8 μ s; (5) 12 μ s, measured in CHCl_3 . (Inset) Steady-state electronic absorption spectra of radical cation of 7MNT in CHCl_3 .

7MTCA and TiO_2 nanoparticles as described in the previous section.

3.3. Transient absorption

The transient absorption spectra of the DA system 7MTCA in CHCl_3 , in the absence and also in the presence of TiO_2 nanoparticles, were measured by direct excitation of ground state CT band at 355 nm, using the third harmonic of Nd:YAG laser system. The spectra are shown in Fig. 9. A transient at 500 nm was found. It is observed from the UV–vis spectral measurements of the product obtained from the electrochemical oxidation of 7MNT that 7MNT cationic band absorbs at 500 nm. The oxidized species of 7MNT has been prepared [31] by constant current charger (model DB 300 DB Electronics, India). The naphthothiophene cation radical, produced by electrochemical oxidation of 7MNT, exhibits electronic absorption band at 500 nm (inset of Fig. 9). Thus, the band observed in the transient spectra of 7MTCA around 500 nm in both the absence and presence of TiO_2 could be logically assigned as the band of radical cation of 7MNT. Methoxy group being an efficient electron donor group undergoes mesomeric interaction with the electron acceptor functionality $-\text{COOH}$ by delocalization of its lone pair of electrons through the aromatic system. Thus as a product of the photoinduced electron-transfer reactions, a radical cationic species (which absorbs at 500 nm) is formed.

The time profiles of the absorption of the cationic species at 500 nm in the absence and also in the presence of TiO_2 nanoparticles are reproduced in Fig. 10. From the decay analysis it appears that the ion-pair lifetime (τ_{ip}) of the cationic species in the triplet state in the presence of TiO_2 is relatively larger (~ 2.03 μ s) than the corresponding value observed in the absence of TiO_2 (~ 1.78 μ s). Thus, from the above observations it appears that the lifetime of the charge-separated species is somewhat enhanced in the presence of TiO_2 nanoparticles.

The yield, ϕ_{R} , of the charge-separated species was obtained from the time profile of the transient absorption band both in absence and presence of TiO_2 nanoparticles. The ϕ_{R} is

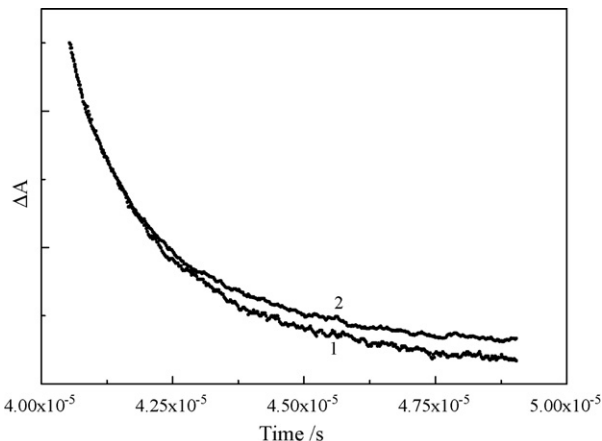


Fig. 10. The time profiles of the absorbance (ΔA) of the cationic bands of 7MTCA (~ 500 nm) in the absence (decay 1) and in the presence (decay 2) of TiO_2 nanoparticles in CHCl_3 .

determined experimentally [40] by taking the ratio of the constant absorbance at long delay times (absorbance mostly due to charge-separated species) and the initial value estimated by extrapolating the ion-absorbance to $t=0$.

The yield ϕ_{R} of the charge-separated species is related with the rate parameters associated with charge recombination (k_{CR}) and charge-separated (k_{CST}) species formation by the first order expression [40]:

$$\tau_{\text{ip}} = \frac{1}{(k_{\text{CR}} + k_{\text{CST}})}$$

$$\phi_{\text{R}} = k_{\text{CST}}\tau_{\text{ip}}$$

The values of ϕ_{R} , τ_{ip} , k_{CR} and k_{CST} of the donor–acceptor system 7MTCA in absence and in presence of TiO_2 nanoparticles are shown in Table 2.

From the observed values it is apparent that charge recombination rate within the present donor–acceptor system 7MTCA has a tendency to slow down with concomitant enhancement of k_{CST} and ϕ_{R} values when TiO_2 is added to the solution of 7MTCA in CHCl_3 . This experimental finding demonstrates that the survival duration of charge-separated species formed within 7MTCA as a product of photoinduced electron-transfer reaction increases in presence of TiO_2 due to retardation of energy destructive charge recombination process.

In the absence of TiO_2 nanoparticles, charge-separated species are formed due to intramolecular electron-transfer between the donor (OCH_3) and acceptor ($-\text{COOH}$) groups of the present DA system. As it is apparent from the UV–vis spectral measurements, the presence of TiO_2 nanoparticles lead to the formation of ground surface complexes between the

Table 2
Changes observed in the values of the parameters ϕ_{R} , τ_{ip} , k_{CR} and k_{CST} of 7MTCA in presence of TiO_2 nanoparticles

Systems	τ_{ip} (μ s)	ϕ_{R}	k_{CR} ($\times 10^5 \text{ s}^{-1}$)	k_{CST} ($\times 10^4 \text{ s}^{-1}$)
7MTCA	1.78	0.09	5.1	5.1
7MTCA + TiO_2	2.03	0.17	4.1	8.4

–COOH group of the DA system and TiO₂ particle. From the present investigation, it seemingly indicates that the formation of ground surface complexes may be responsible for the enhancement of the longevity of the charge-separated species by reducing the back electron-transfer rate. It is possible that due to the strong binding of carboxylate group (–COOH) with TiO₂, the overlapping integral between the group and the rest electron rich site, i.e., donor part 7MNT of the molecule 7MTCA should be decreased resulting in reduction of recombination rate processes. Thus, in the present investigation TiO₂ appears not to act as an acceptor but its participation in the strong complex formation with the –COOH group of 7MTCA helps to survive or protect the charge-separated species formed within this organic DA compound 7MTCA due to photoinduced intramolecular electron-transfer reactions between the donor (OCH₃) and acceptor functionalities (–COOH) present in it. The non-participation of TiO₂ as an acceptor is further confirmed from the electrochemical measurements which have been described below.

The oxidation and reduction potentials of 7MTCA, estimated from the cyclic voltammetry (details are given in Section 2.5), are found to be +0.45 and –0.98 V, respectively. According to the earlier observations [31], the oxidation potential should be due to the presence of the donor part (functionality) containing methoxy group (–OCH₃) and the reduction potential should be due to the acceptor part carboxylate group (–COOH). The energy of conduction band of TiO₂, measured from cyclic voltammetry, is –1.1 V. Since the one electron reduction potential of the acceptor part of 7MTCA is less negative than conduction band of TiO₂, electron-transfer from the donor part of 7MTCA to TiO₂ is thermodynamically unfavorable. However, further investigations are underway on other naphthothiophene type rigid molecular systems using TiO₂ nanoparticles. From the present experimental findings of enhancement of survival duration of charge-separated species, formed within 7MTCA, in presence of TiO₂ nanoparticles due to retardation of energy wasting charge recombination process, it reveals that hetero-supramolecular assemblies for solar-energy conversion devices, e.g., low-cost organic photovoltaic cells [41, 1 and references therein] could possibly be designed with 7MTCA (or similar simple naphthothiophene compounds having the electron donor and acceptor functionalities) and TiO₂ nanoparticles, of which the former organic molecule should be attached with the TiO₂ core. Synthesis of such systems is underway.

4. Concluding remarks

Both steady-state and time-resolved spectroscopic measurements demonstrate the formations of charge-separated species both in the excited singlet and triplet states due to the photoinduced intramolecular electron-transfer between the donor (–OCH₃) and acceptor (–COOH) functional groups of 7MTCA. The presence of TiO₂ nanoparticles does not retard the forward electron-transfer process within 7MTCA but instead the decay kinetics of the cationic band observed from the transient absorption spectra shows the enhancement of the lifetime of the charge-separated species in the presence of TiO₂ nanoparticles,

i.e., the radical ion-pair formed within 7MTCA is protected due to strong binding between the carboxylate group, –COOH and the TiO₂ nanoparticles. Thus, in the present investigation TiO₂ appears not to act as an acceptor but through formation of strong complex, as evidenced from FT-IR measurements, with –COOH functionality of the organic molecule 7MTCA helps to survive or protect the charge-separated species formed within this compound. The possibility of building up of low cost artificial solar energy conversion devices (e.g., photovoltaic cells) by attaching the DA system 7MTCA with the TiO₂ core is predicted.

Acknowledgments

We thankfully acknowledge the cooperation of Professor Sanjib Ghosh of Chemistry Department of Presidency College, Kolkata, India for providing us the facility, sponsored by the Department of Science and Technology (DST), New Delhi, India, for fluorescence lifetime measurements. We thank Professor Samita Basu of Saha Institute of Nuclear Physics, Kolkata, India for helping in the measurements of transient absorption spectra and decays with the help of nanosecond laser flash photolysis set-up. Thanks are due to Mr. Supriya Chakraborty of MLS Department for the measurements of the size of the TiO₂ nanoparticles by using transmission electron micrograph (TEM). TG acknowledges the financial support provided by the Department of Science and Technology (DST) (project no. SR/S1/PC-17/2003), New Delhi, India in the form of grants and fellowships.

References

- [1] T. Hasobe, S. Hattori, P.V. Kamat, Y. Wada, S. Fukuzumi, *J. Mater. Chem.* 15 (2005) 372.
- [2] R.A.J. Janssen, W.J.E. Beek, *J. Mater. Chem.* 14 (2004) 2795.
- [3] Handbook of Organic–Inorganic Hybrid Materials and Nanocomposites, in: H.S. Nalwa (Ed.), American Scientific Publishers, Stevenson Ranch, California, 2003.
- [4] C. Sanchez, B. Lebeau, F. Chaput, J.P. Boilot, *Adv. Mater.* 15 (2003) 1969.
- [5] J.W. Kriesel, T.D. Tilley, *Adv. Mater.* 13 (2001) 1645.
- [6] K.E. Gonsalves, L. Merhari, H. Wu, Y. Hu, *Adv. Mater.* 13 (2001) 703.
- [7] (a) B. O'Regan, M. Grätzel, *Nature* 353 (1991) 737;
(b) U. Bach, D. Lupo, P. Comte, J.E. Moser, F. Weissörtel, J. Salbeck, H. Spreitzer, M. Grätzel, *Nature* 395 (1998) 583.
- [8] (a) R.A.J. Janssen, W.J.E. Beek, *Adv. Funct. Mater.* 12 (2002) 519;
(b) V.L. Colvin, M.C. Schlamp, A.P. Alivisatos, *Nature* 370 (1994) 354.
- [9] M.C. Schlamp, X. Peng, A.P. Alivisatos, *J. Appl. Phys.* 82 (1997) 5837.
- [10] H. Mattoussi, L.H. Radzilowski, B.O. Dabbousi, E.L. Thomas, M.G. Bawendi, *J. Appl. Phys.* 83 (1998) 7965.
- [11] W.U. Huynh, X. Peng, A.P. Alivisatos, *Adv. Mater.* 11 (1999) 923.
- [12] D.C. Ginger, N.C. Geenham, *Phys. Rev. B* 59 (1999) 10622.
- [13] K.S. Narayan, A.G. Manoj, J. Nanda, D.D. Sarma, *Appl. Phys. Lett.* 74 (1999) 871.
- [14] J. Lee, V.C. Sundar, M.G. Bawendi, K.F. Jensen, *Adv. Mater.* 12 (2000) 1102.
- [15] (a) A.N. Shipway, I. Willner, *Chem. Commun.* 20 (2001) 2035;
(b) A. Hagfeldt, M. Grätzel, *Acc. Chem. Res.* 33 (2000) 269.
- [16] M. Hilgendorff, V. Sundström, *J. Phys. Chem. B* 102 (1998) 10505.
- [17] J. Pan, G. Benkö, Y. Xu, T. Pascher, L. Sun, V. Sundström, T. Polivka, *J. Am. Chem. Soc.* 124 (2002) 13949.
- [18] J. He, G. Benkö, F. Korodi, T. Polivka, R. Lomoth, B. Akermark, L. Sun, A. Hagfeldt, V. Sundström, *J. Am. Chem. Soc.* 124 (2002) 4922.

- [19] A.F. Nogueira, M.A. De Paoli, I. Montanari, R. Monkhouse, J. Nelson, J.R. Durrant, *J. Phys. Chem. B* 105 (2001) 7517.
- [20] G. Benkő, M. Hilgendorff, A.P. Yartsev, V. Sundström, *J. Phys. Chem. B* 105 (2001) 967.
- [21] X. Marguerettaz, D. Fitzmaurice, *J. Am. Chem. Soc.* 116 (1994) 5017.
- [22] X. Marguerettaz, R. O'Neil, D. Fitzmaurice, *J. Am. Chem. Soc.* 116 (1994) 2629.
- [23] X. Marguerettaz, G. Redmond, S.N. Rao, D. Fitzmaurice, *Chem. Eur. J.* 2 (1996) 420.
- [24] L. Cusack, S.N. Rao, J. Wenger, D. Fitzmaurice, *Chem. Mater.* 9 (1997) 624.
- [25] X. Marguerettaz, A. Merrins, D. Fitzmaurice, *J. Mater. Chem.* 8 (1998) 2157.
- [26] A. Merrins, X. Marguerettaz, S.N. Rao, D. Fitzmaurice, *Chem. Eur. J.* 7 (2001) 1309.
- [27] S. Pelet, M. Grätzel, J. Moser, *J. Phys. Chem. B* 107 (2003) 3215.
- [28] S. Hattori, T. Hasobe, K. Ohkubo, Y. Urano, N. Umezawa, T. Nagano, Y. Wada, S. Yanagida, S. Fukuzumi, *J. Phys. Chem. B* 108 (2004) 15200.
- [29] A. Furube, R. Katoh, T. Yoshihara, K. Hara, S. Murata, H. Arakawa, M. Tachiya, *J. Phys. Chem. B* 108 (2004) 12583.
- [30] S. Hattori, K. Ohkubo, Y. Urano, H. Sunahara, T. Nagano, Y. Wada, N.V. Tkachenko, H. Lemmetyinen, S. Fukuzumi, *J. Phys. Chem. B* 109 (2005) 15368.
- [31] S.K. Pal, T. Sahu, T. Misra, T. Ganguly, T.K. Pradhan, A. De, *J. Photochem. Photobiol. A: Chem.* 174 (2005) 138.
- [32] N.A. Kotov, F.C. Meldrum, J.H. Fendler, *J. Phys. Chem.* 89 (1994) 8827.
- [33] B. Enright, D. Fitzmaurice, *J. Phys. Chem.* 100 (1996) 1027.
- [34] K. Kalyanasundaram, M. Grätzel, *Coord. Chem. Rev.* 77 (1998) 347.
- [35] D. Duonghong, J. Ramsdan, M. Grätzel, *J. Am. Chem. Soc.* 104 (1982) 2977.
- [36] J. Kawakami, H. Itoh, H. Mitsuhashi, S. Ito, *Anal. Sci.* 15 (1999) 617.
- [37] M. Maiti, T. Misra, T. Bhattacharya, C. Basu, A. De, S.K. Sarkar, T. Ganguly, *J. Photochem. Photobiol. A: Chem.* 152 (2002) 41.
- [38] L.P. Zang, B. Chen, L.Z. Wu, C.H. Tung, H. Cao, Y. Tanimato, *J. Phys. Chem. A* 107 (2003) 3438.
- [39] T. Sahu, S.K. Pal, T. Misra, T. Ganguly, *J. Photochem. Photobiol. A: Chem.* 171 (2005) 39.
- [40] T. Ganguly, D.K. Sharma, S. Gauthier, D. Gravel, G. Durocher, *J. Phys. Chem.* 96 (1992) 3757.
- [41] S. Fukuzumi, H. Kotani, K. Ohkubo, S. Ogo, N.V. Tkachenko, H. Lemmetyinen, *J. Am. Chem. Soc.* 126 (2004) 1600.